Talanta 105 (2013) 235–243

Contents lists available at SciVerse ScienceDirect

Talanta

journal homepage: www.elsevier.com/locate/talanta

Elemental mapping in fossil tooth root section of *Ursus arctos* by laser ablation inductively coupled plasma mass spectrometry (LA-ICP-MS)

M. Vašinová Galiová [a,b], M. Nývltová Fišáková [c], J. Kynický [d], L. Prokeš [a], H. Neff [e], A.Z. Mason [f], P. Gadas [g], J. Košler [h], V. Kanický [a,b,*]

[a] Department of Chemistry, Faculty of Science, Masaryk University, Kotlářská 2, 611 37 Brno, Czech Republic
[b] Central European Institute of Technology (CEITEC), Masaryk University, Kamenice 5, 625 00 Brno, Czech Republic
[c] Institute of Archaeology, The Academy of Sciences of the Czech Republic, Královopolská 147, 612 00 Brno, Czech Republic
[d] Department of Geology and Pedology, Faculty of Forestry and Wood Technology, Mendel University in Brno, Zemědělská 3, 613 00 Brno, Czech Republic
[e] Department of Anthropology and Institute for Integrated Research in Materials, Environments, and Society (IIRMES), California State University Long Beach, Bellflower Blvd 1250, 90840 Long Beach, USA
[f] Department of Biological Sciences, California State University Long Beach, Bellflower Blvd 1250, 90840 Long Beach, USA
[g] Department of Geological Sciences, Faculty of Science, Masaryk University, Kotlářská 2, 611 37 Brno, Czech Republic
[h] Centre for Geobiology, University of Bergen, P.O. Box 7803, N-5020 Bergen, Norway

ARTICLE INFO

Article history:
Received 30 August 2012
Received in revised form
10 December 2012
Accepted 13 December 2012
Available online 31 December 2012

Keywords:
Laser ablation ICP-MS
Geochemical analysis
Migration
Diet
Diagenesis

ABSTRACT

Laser ablation inductively coupled plasma mass spectrometry (LA-ICP-MS) was used to map the matrix (Ca, P) and trace (Ba, Sr, Zn) elements in the root section of a fossilized brown bear (*Ursus arctos*) tooth. Multielemental analysis was performed on a (2.5×1.5) cm^2 area. For elemental distribution, a UP 213 laser ablation system was coupled either with a quadrupole or a time of flight ICP-MS. The cementum and dentine on the slice of the sample surface were clearly distinguishable, especially changes in elemental distribution in the summer and winter bands in the fossil root dentine. Migration and diet of *U. arctos* were determined on the basis of fluctuations in Sr/Zn ratio and their contents. Quantification was accomplished with standard reference material of bone meal (NIST 1486) and by the use of electron microprobe analysis (EMPA). Changes in Sr/Zn and Sr/Ba ratios relating to the season, and composition of food during the lifetime of the animal are discussed on basis of analysis of light stable isotopes. It was observed that there was an increase in the Sr/Zn ratio during the winter season caused by a reduction of food intake during hibernation. Above mentioned inferences drawn from elemental data obtained by LA-ICP-MS were confirmed independently by determination of carbon, nitrogen and strontium isotopes. Moreover, diagenesis and its interfering influence on the biogenic composition of cementum and dentine were resolved. According to the distribution and/or content of the element of interest, post-mortem alterations were revealed. Namely, U, Na, Fe, Mg and F predicate about the suitability of the selected area for determination of migration and diet.

1. Introduction

The main components of bones and teeth are calcium and phosphorus in the form of hydroxyapatite ($Ca_{10}(OH)_2(PO_4)_6$) and represent 39.9%$_{m/m}$ Ca and 18.5%$_{m/m}$ P of the mineral-phase. Strontium, barium, zinc, copper, vanadium, manganese or magnesium and sodium occur as the trace and minor elements. Non-mineral constituents include collagen, marrow, fat, non-collagen proteins and water.

The tooth consists of a number of structurally different mineralized parts; enamel, dentine and cementum. Enamel, the hardest skeletal tissue in the body, covers the crown and begins to form during pregnancy. Its composition reflects the diet in childhood [1]. Dentine is a metabolically active tissue and its composition is constantly renewed, thus dentine analysis provides information about dietary system 10 years prior to the death. Moreover, skeletal tissue composition can provide information on geographical origin. Strontium, calcium, zinc and barium analyses can be used to determine provenance and dietary history. Strontium has a similar ionic radius and charge to Ca and presumably enters into plants *via* the Ca^{2+} permeases nutrient pathway. Plants can subsequently be consumed by animals/human and become incorporated into mineralized structures [2]. The lowest strontium content is found in meat and subsequently in the skeletal remains of carnivores. In contrast, a higher content of Sr has been found in bioapatite structures of herbivores [2]. The highest Sr content in bones and teeth has been identified in animals/human with a seafood diet. The partitioning

* Corresponding author at: Department of Chemistry, Faculty of Science, Masaryk University, Kotlářská 2, 611 37 Brno, Czech Republic.
E-mail address: viktork@chemi.muni.cz (V. Kanický).

0039-9140/$ - see front matter © 2013 Elsevier B.V. All rights reserved.
http://dx.doi.org/10.1016/j.talanta.2012.12.037

between Ca and Sr according to dietary sources enables Sr/Ca ratios to be used as a proxy for determining diet and migration [3–5]. The reconstruction of dietary history can be also performed *via* the Zn content and Sr/Zn ratio. The lowest amount of Zn in skeletal tissue occurs in herbivores, increasing through omnivores and is highest in carnivores. A high amount of Zn in teeth, however, might indicate inflammation in skeletal tissue or surroundings area [6]. According to the literature, barium is more sensitive than zinc as an indicator of changes in diet and Sr/Ba ratios enable terrestrial and marine dietary sources to be distinguished [7–9].

Migration of individuals is ordinarily determined by undertaking strontium isotope analysis ($^{87}Sr/^{86}Sr$) of enamel and dentine or bone tissue. The $^{87}Sr/^{86}Sr$ in this mineralized structure reflects the strontium isotopic compositions in the surrounding environment and can therefore be used to determine geographical location [10]. Isotopic ratios of Sr are well defined for geological background and sea/fresh water as well. For instance, sea water is characterized by lower $^{87}Sr/^{86}Sr$ isotopic ratios and is higher where the influence of sea water is diminished [11,12].

The conclusions drawn from elemental analyses can be confirmed by the $^{13}C/^{12}C$ ratio ($\delta^{13}C$). Differences in the ratio occur between C3 and C4 plants and their carbohydrate products [13,14]. C3 plants encompass grass, temperate trees, fruit trees, rice, and most cereals and root vegetables. C4 plants include tropical/subtropical grasses, maize, millet, sugarcane and sorghum. Nitrogen isotopes ($^{15}N/^{14}N$ – $\delta^{15}N$) are also useful for determining trophic standing and the distinguishing between terrestrial and marine diets and those composed primarily of plants or meat [15,16].

In the case of fossil samples, trace and minor elemental content can be influenced by diagenesis. Diagenesis causes either enrichment and/or loss of elements depending on the composition of the soil, pH, and environmental conditions, e.g. [17]. The processes involved in diagenesis are poorly understood. The early phase of diagenesis of mineralized structures is probably correlated with an initial decrease in the collagen matrix [18]. Subsequently, changes in bones and teeth composition occur. It is well known that the content of fluorine ions is directly proportional to age of fossil sample. Fluorine gets incorporated into the structures of hydroxyapatite and replaces hydroxyl groups [19]. Similar behavior has been described for CO_3^{2-}, Cl^- or H_2O. Over time, the content of water and OH^- decreases as fossilization progresses [20]. The phosphate group is, in comparison with the hydroxyl component, more resistant to diagenetic change [21]. However, substitution by CO_3^{2-} has been observed [20]. Cationic changes are also evident during diagenesis. Magnesium, sodium and strontium can replace Ca in the hydroxyapatite structure and diagenesis is also typically characterized by elevated content of iron, manganese, silicon, aluminum and barium [20]. In the case of iron, manganite and smectite can be present $[(Fe^{3+}Mn^{3+})O(OH)]$ [21]. Moreover, increased content of rare earth elements (REE) and U is connected with alteration of the hydroxyapatite [22].

The changes in composition of teeth have been investigated by various methods (XRD — X-ray diffraction, IR — infrared spectroscopy, PIXE — proton induced X-ray analysis, EMPA — electron microprobe analysis, SIMS — secondary ion mass spectrometry and LA-ICP-MS — laser ablation inductively coupled plasma mass spectrometry, etc.) [23–27].

Of these techniques, LA-ICP-MS is becoming increasingly popular because of its speed and ease of use. The technique provides relatively high spatial resolution on the scale of several micrometers, permits scanning of the sample surface and can be used to obtain two-dimensional maps of elemental distribution. There are other benefits such as low detection limits important in trace and ultra-trace analysis, multielemental analysis, minimization of risk of contamination and loss of volatile elements during decomposition of sample and minimal or no samples preparation is required. The procedure has been used in archeology [28–30], biology [31] and geology, [32] for a variety of applications, from simple elemental mapping [33–36], bioimaging of soft [37–41] and hard [42,43] tissue or for determination of origin [44] and dating [45].

Quantitative LA-ICP-MS is not a routine procedure and most samples require individualized processing on a case to case basis for accurate quantitative analysis. One of the major issues is the lack of appropriate standard reference materials for the preparation of calibration standards for bias-free, matrix-matched calibration. In some cases, calibration can be achieved by generating matrix-matched laboratory standard materials pressed into the pellets. However, even in these cases, differences in the hardness, optical properties etc. of the matrix in the standard and sample may cause differences in ablation rates, aerosol particle size distributions, aerosol transport, evaporation, atomization, ionization and hence in sensitivities. These processes can lead to non-stoichiometric ablation and elemental fractionation during analysis, causing false elemental signal ratios and analytical inaccuracies [46–51]. An empirical approach to correct for differences in signal sensitivities between analyzed samples and calibration standards is to incorporate an internal standard signal. Generally, element selected as an internal standard has to be incorporated homogeneously and its concentration independently validated by means of an alternative quantitative procedure [52]. The normalization to the sum of all components to $100\%_{m/m}$ represents another possibility [53].

Individual types of mass spectrometers differ in their advantages and limitations and therefore, the selection of an appropriate analyzer for a specific application is important. Strontium isotopic ratio measurements require precision on the level of 10^{-3}% [54], which is best served using a multicollector – inductively coupled plasma mass spectrometer (MC-ICP-MS) [55]. Single collectors (e.g., quadrupole and time of flight analyzers) do not exhibit the same level of precision but have superior workflow throughput, are more versatile, are less expensive and can be used for simpler application, such as elemental distribution in simple matrices. Additionally, quadrupole instruments equipped with collision and reaction cells help to reduce polyatomic interferences, which are an important consideration when analyzing calcified tissue, which has a complex matrix characterized by many interferences that influence accuracy of determination of both major and minor elements [56].

The aim of this study is to assess the ability of LA-ICP-MS with quadrupole and time of flight analyzers to reconstruct the diet and migration pattern of a prehistoric brown bear by analyzing the distribution of minor and trace elements (zinc, barium, strontium, sodium, uranium e.g.) and matrix components (calcium and phosphorus) in the dentine of a fossilized tooth. The utility of Sr/Zn and Sr/Ba ratios to deduce changes in diet and geographical location is discussed. Calibration of the LA-ICP-MS was facilitated by results obtained with EMPA. Migration and dietary inputs were validated by using nitrogen, carbon and strontium isotopes. Diagenesis was investigated by studying content changes between cementum and dentine. Differences were observed towards the root channel of the fossilized tooth.

2. Experimental

2.1. Laser ablation inductively coupled plasma quadrupole mass spectrometry instrumentation, LA-ICP-(Q)MS

Analyses were conducted using an Agilent 7500ce (Agilent Technologies, Santa Clara, CA, USA) quadrupole ICP-MS with an attached UP 213 laser ablation system (New Wave Research, Inc., Fremont, CA, USA). The sample was placed into a SuperCell (New Wave Research, Inc., Fremont, CA, USA) having volume of 33 cm^3

and ablated using a commercial Q-switched Nd:YAG laser operated at a wavelength of 213 nm (pulse duration 4.2 ns). An XY-stage was used to move the sample along a programmed trajectory and a CCD camera was used to monitor the ablation event. Ablated material was transported from the sample chamber using helium carrier gas (1 l min^{-1}) and mixed with argon (0.6 l min^{-1}) prior to the torch. Optimization of LA-ICP-MS parameters (gas flow rates, sampling depth, voltage of ion optics) was performed using glass reference material NIST SRM 612 to maximize the S/N ratio and minimum oxide formation (ThO^+/Th^+ counts ratio 0.2%) and U^+/Th^+ counts ratio 1.1%.

All laser ablation based measurements were performed with a laser fluence of 12 J cm^{-2}. Laser frequency was 20 Hz and 10 Hz for line scanning and spot analysis, respectively. ^{23}Na, ^{24}Mg, ^{57}Fe, ^{86}Sr, ^{88}Sr, ^{135}Ba and ^{238}U isotopes were measured using an integration time of 0.1 s/isotope; ^{43}Ca, ^{44}Ca and ^{31}P were recorded using an integration time of 0.05 s/isotope.

2.2. Laser ablation inductively coupled plasma time-of-flight mass spectrometry instrumentation, LA-ICP-(TOF)MS

Laser ablation experiments conducted with time-of-flight mass spectrometry were performed at the Department of Biological Sciences, California State University Long Beach, an institution collaborating *via* the project Laser Ablation with Inductively Coupled Plasma Spectrometry and Laser Induced Breakdown Spectroscopy in archaeology and anthropology ME10012, supported by Ministry of Education, Youth and Sports of the Czech Republic and AMVIS (American Science Information Centre, Prague, Czech Republic).

Analyses were performed using a GBC Optimass 8000 time-of-flight ICP-MS with orthogonal ion optics. Laser sampling was accomplished using a laser ablation system UP 213 using settings similar to those used for the quadrupole analyses. Signal intensities for the selected analytes were collected in five 1 s integrations, each of which recorded 30,000 spectra. A delay time of 8 s preceded collection of signal intensities. Gas flow and torch position were optimized at the beginning of each day using NIST SRM 612. Standards were run approximately every half hour during the course of the analysis. Intensities of isotopes were obtained using a laser fluence of 5 J cm^{-2} at a frequency of 20 Hz.

2.3. Electron microprobe analysis

The chemical composition of the root section was determined using a Cameca SX100 electron microprobe at Joint Laboratory of Electron Microscopy and Microanalysis, Department of Geological Sciences, Masaryk University, Brno and The Czech Geological Survey, Brno. The instrument was operated at an accelerating voltage of 15 kV, a beam current of 10 nA and a beam size of 10 μm. The following calibration standards and analytical lines were used: (Kα) lines: albite (Na), almandine (Si), grossular (Al), Mg_2SiO_4 (Mg), fluorapatite (Ca, P), sanidine (K), NaCl (Cl), hematite (Fe), gahnite (Zn), topaz (F); (Lα) lines: $SrSO_4$ (S, Sr), baryte (Ba). The peak counting times ranged from 10–30 s for all elements except for Sr (60 s). The average detection limits and standard deviations (in parentheses) under these conditions were: ~1200 mg kg^{-1} (0.14) for Ba; ~1200 mg kg^{-1} (0.13) for F; ~1000 mg kg^{-1} (0.1) for Zn and Sr; ~700 mg kg^{-1} (0.64) for Ca; ~700 mg kg^{-1} (0.12) for Na; ~500–600 mg kg^{-1} (0.04–0.08) for S and Fe; ~400 mg kg^{-1} (0.4) for P and ~200–300 mg kg^{-1} (0.02–0.04) for Si, Al, Mg, K, Cl. The analytical data were corrected using the PAP correction procedure [57].

2.4. Samples and sample preparation

The bear canine tooth analyzed in this paper (Fig. 1) was excavated in 1986 at Dolní Věstonice and originated from a brown bear (*Ursus arctos*). It was excavated from the field II, which is a longitudinal zone on top of the site, adjacent to the triple burial area. Abrasion of the tooth's oclusal area and seasonal cementum increments of tooth's root were used to determine that the animal died between August–October and was approximately 14 years old at death.

Dolní Věstonice II is one of a series of large settlements of mammoth hunters on the loess elevations at altitudes of about 180–240 m a.s.l., rising above the Dyje River and sloping further to the top of the Pavlovské vrchy in Moravia (the eastern part of the Czech Republic). Archeological excavations at this site were organized by Klíma and Svoboda between 1985 and 1989, and additional excavations took place in 1991, 1999 and 2005 [58,59]. The site is world-famous for human paleontological finds including the triple burial discovered at the top of the site, the old man burial on the western slope, and individual human remains scattered at various places in the cultural layer. The site probably had repeated occupations, extended over a timespan of 32,000 years (ka) before present (BP) to 28.5 ka BP (^{14}C). This timespan is framed by a series of earlier and later luminescence dates from paleosols and loess below and above, which make Dolní Věstonice II the best dated Gravettian site in the region.

For carbon and nitrogen isotopic analysis of collagen was performed at Czech Geological Survey. The tooth was cleaned using an ultrasonic bath, dried, gently crushed into small fragments and then treated with diluted 1 mol l^{-1} acetic acid to

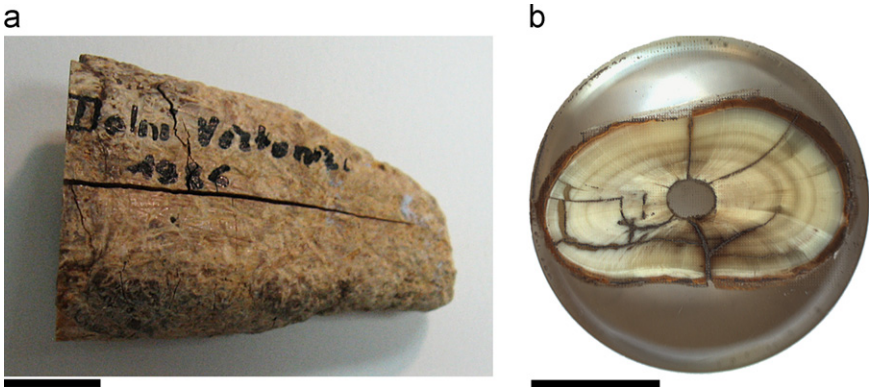

Fig. 1. Photographs: (a) of the bear canine tooth sample excavated at Dolní Věstonice and (b) of the studied sample surface, embedded in resin, with ablation pattern. The bar has a length of 1 cm.

remove surface impurities and secondary carbonates. Periodic evacuation ensured that evolved carbon dioxide was removed from the interior of the samples fragments, and that fresh acid was allowed to reach even the interior micro-surfaces. The chemically cleaned sample was then reacted under vacuum with 1 mol l^{-1} HCl to release carbon dioxide from the bioapatite. The residue was filtered, rinsed with deionised water and, under slightly acid condition (pH=3), heated to 80 °C for 6 h to dissolve the collagen and leave humic substances in the precipitate. The collagen solution was then filtered and dried to isolate pure collagen which was then combusted at 575 °C in an evacuated/sealed Pyrex ampoule in the presence of CuO. The values $\delta^{13}C$ and $\delta^{15}N$ were measured using a MAT 251 Finnigan mass spectrometer and expressed as $\delta^{13}C$ with respect to PDB (PeeDee Belemnite), with an error of less than 0.1‰, and as $\delta^{15}N$ with respect to atmospheric nitrogen with an error of less than 0.2‰ [60].

Sr isotopic analysis conducted at University of Bergen was performed following the complete dissolution of approximately 0.1 g of powdered tooth sample in 10 ml of concentrated HNO_3 in an ETHOS One (Milestone S.r.l., Italy) microwave oven. The resulting solution was diluted with water to achieve a final HNO_3 concentration of 3 mol l^{-1}. Ion-exchange chromatography using a Sr-spec column (Eichrom Technologies, Inc., IL, USA) was employed to isolate Sr from the sample matrix. Strontium isotopes were measured with a Finnigan MAT 262 thermal ionization mass-spectrometer equipped with an array of 9 faraday detectors. Sr isotopes (masses 84, 86, 87 and 88) and interfering Rb (masses 85 and 87) were measured in a static mode from a double Re filament. The isotopic ratios were corrected for mass-dependent fractionation using $^{86}Sr/^{88}Sr=0.1194$ and exponential law, and Rb interference. Repeat measurements of the NBS-987 standard over the course of the study gave a mean $^{87}Sr/^{86}Sr$ value of 0.710247 ± 0.000007 (2 sigma). Long term precision measurements of the Sr isotopic composition of a NBS-987 standard were 0.04‰. NIST SRM 1486 bone meal powder was also analyzed during this study and gave an $^{87}Sr/^{86}Sr$ value of 0.709274 ± 0.000008 (2 sigma).

3. Results and discussion

3.1. Strontium isotopic ratio

A $^{87}Sr/^{86}Sr$ value of 0.710029 ± 0.000007 (2 sigma) was measured from the enamel of the *U. arctos* canine excavated from Dolní Věstonice II. This value differs from the isotopic ratio characterizing geological locality of the Dolní Věstonice II, which was determined to range from 0.708914 to 0.709794 based upon the analysis of a garden snail shell (*Helix pomatia*), implying that the bear was not from this location. The observed Sr isotopic signature of the tooth more closely resembled that of the Krumlov forest and Moravian Karst, which have Sr ratios of 0.7108–0.7115 [61] and 0.710010–0.710540 (unpublished data), respectively, indicating that the animal had either migrated to the Palava region or had been captured in the Krumlov forest and Moravian Karst and subsequently transported to Dolní Věstonice. The Moravian Karst lies approx. 70 km from Dolní Věstonice. The brown bear's territory was approximately (30–40) km^2. However, the bear can sometimes migrate for more than 100 km [62,63].

3.2. Carbon and nitrogen isotopic ratio

Carbon and nitrogen ($^{13}C/^{12}C$ a $^{15}N/^{14}N$) isotopic ratio analyses conducted on the tooth to identify the bear's diet and palaeoenvironment provided data that was outside the variation range known for brown bears from the Pleistocene and Holocene epochs [64,65] (Table 1). The elevated content of ^{15}N isotope in the tooth could mean the bear either ate flesh-rich diet including freshwater fish or a diet of xeritic plants [66] originating from a rather dry environment comparable to those found in the Moravian Karst region. This latter proposition is supported by the ^{13}C isotope content which indicates that the bear lived on grass steppes, open forests and tundra [66]. Such an environment was thought to exist in the Moravian Karst area during the Gravettian period (i.e. 26 ka BP).

3.3. Comparison of line scanning and spot analysis obtained by quadrupole and time-of-flight analyzers

LA-ICP-MS and EMP analyses were performed on a polished section of a tooth slice taken after embedding in resin (Fig. 1a and b). Time-resolved line scanning analyses across the middle of

Table 1
Carbon and nitrogen isotope ratio in canine tooth of the studied brown bear.

Locality	Tooth	Species	$\delta^{13}C$ (‰)	$\delta^{15}N$ (‰)	N (%)	C/N	C (%)
Dolní Věstonice II–1987	Canine	*Ursus arctos*	−20.2	13.0	15.1	2.9	43.4

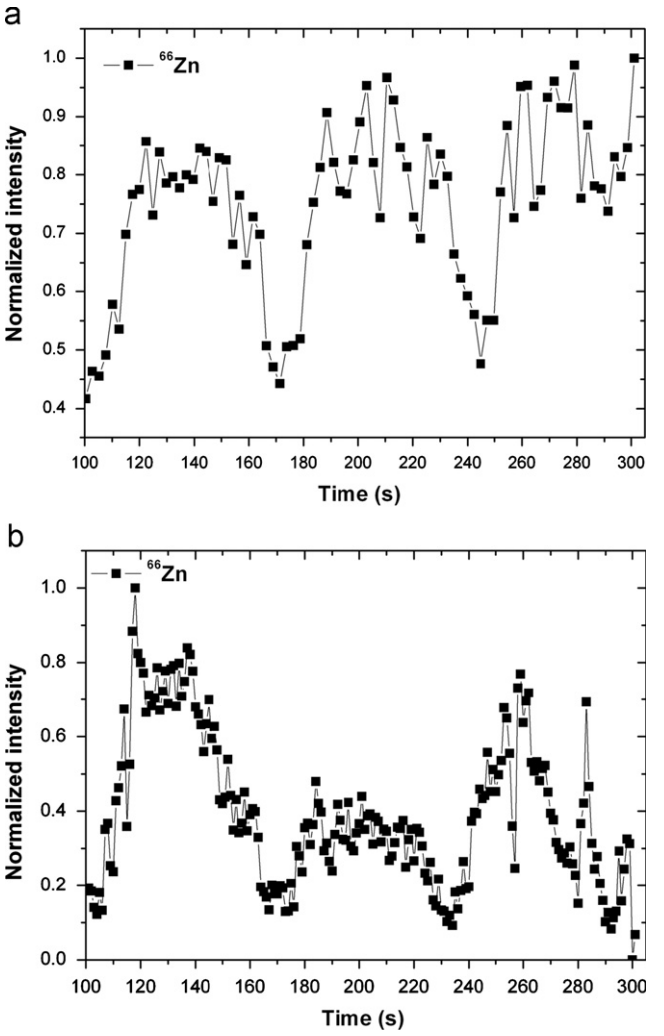

Fig. 2. LA-ICP-MS signal of ^{66}Zn isotope obtained by using (a) quadrupole and (b) time of flight analyzers using line scanning mode. Intensities are normalized to a maximum value.

the root section were performed by both quadrupole and time-of-flight based ICP-MS using a 50 μm diameter ablation spot scanned at a speed of 25 μm s^{-1} at a frequency 20 Hz. Fig. 2 shows changes in the intensity of ^{66}Zn normalized to the maximum intensity value. In general, the overall spatial trends in the intensity of ^{66}Zn observed using the two types of analyzer were similar, as were the Sr/Zn ratios (Fig. 3) despite the lower mass/time resolution of the quadrupole system. The Sr/Zn ratios showed a distinct annual periodicity with spikes every ~2 mm resulting from a decrease of ratio in the winter periods (dark strips in Fig. 1) during hibernation when food intake was low. Similar trends (not shown) were obtained for other ratios (Sr/Ca and Sr/Ba) although these were not as sensitive dietary indicators as the Sr/Ba ratios [30]. This probably relates to the susceptibility of barium to undergo diagenesis relative to zinc [21].

In order to avoid the significant ablation overlap (97.5%) and memory effects that occur in line scan mode, the laser was used in a "discrete spot mode" where ablation craters of 100 μm diameter were separated by 200 μm distances. Moreover, laser sampling using line scanning mode leads to larger particle size and higher matrix effect [47]. Laser pulse-sample surface interaction took about 6 s for each spot, with a 10 s flushing time to allow for a decrease in signal concordant with a reduction in number of pulses from 20 to 10 Hz. These spatial mapping parameters were sufficient to observe spatial changes in elemental distribution

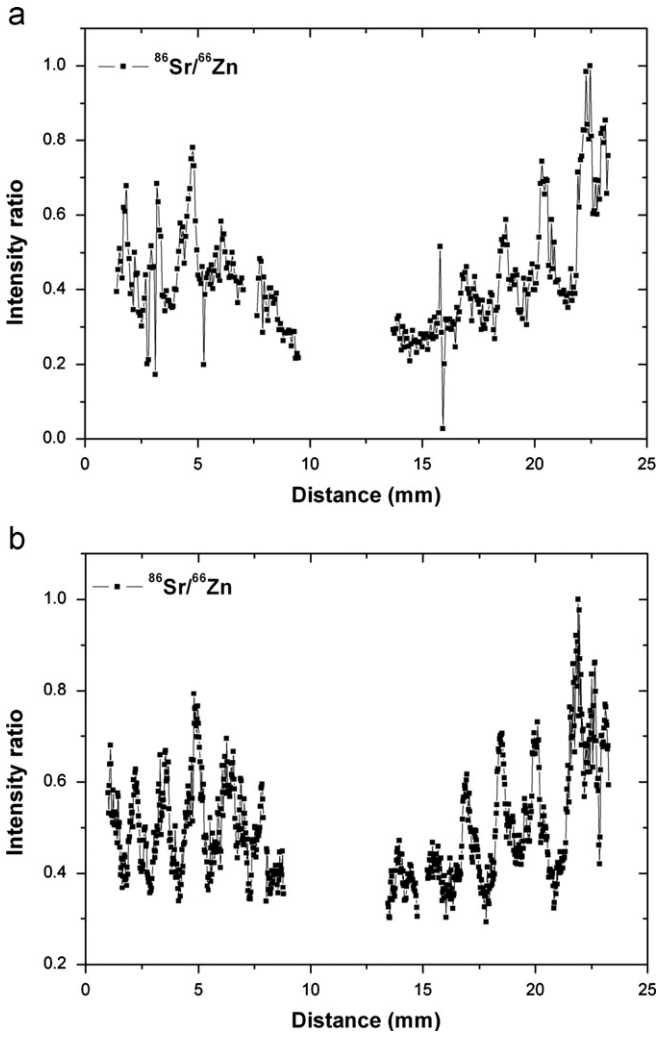

Fig. 3. Intensity ratio of $^{86}Sr/^{66}Zn$ normalized to maximum value obtained by using (a) quadrupole and (b) time of flight analyzers in line scanning mode.

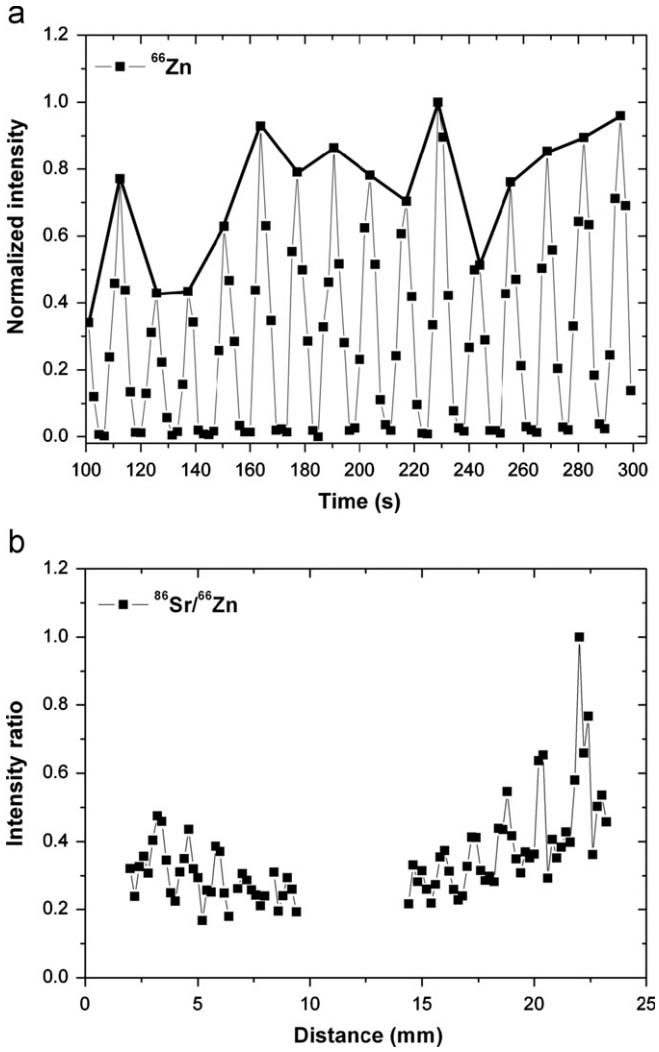

Fig. 4. Typical (Q)MS signal of (a) ^{66}Zn and (b) intensity ratio of $^{86}Sr/^{66}Zn$ recorded during ablation of individual spots. All intensities are normalized to a maximum value. The black bold line marks the distribution of ^{66}Zn in the investigated sample surface.

using quadrupole based mass spectrometry (Fig. 4a). Each ^{66}Zn intensity maximum corresponds to an individual spot analysis with the black bold line describing the distribution of zinc inside the sample surface. Periodic fluctuations of $^{86}Sr/^{66}Zn$ were clearly visible like with line scanning mode (Fig. 4b). Error in analysis was about 7–10% [30] and primarily resulted from the presence of small cavities inside the tooth sample and the inherent error of laser ablation technique itself.

3.4. Elemental mapping and quantification

Two-dimensional elemental mapping of the entire area of the bear canine root section was performed by LA-ICP-(Q)MS in the "discrete spot mode" at a spatial resolution of 200 μm. The data were visualized by GRAMS software [67] after background subtraction, matrix correction and calculation of elemental content.

The elemental composition of the root part of the fossil tooth investigated by LA-ICP-MS was quantified using compressed bone meal (SRM NIST 1486) as a calibration material. The bone meal corresponds to composition of recent bones, consisting of 26.58%$_{m/m}$ Ca, 12.30%$_{m/m}$ P and other elements. The fossil bones and teeth can have a higher and/or lower content of elements of interest; nevertheless, trends in elemental contents within tooth section could be distinguished using the bone meal [42,43,68].

Differences in the ablation characteristics of the tooth and the pellet were compensated for by normalizing the elemental content to the content of calcium. Content of Ca inside the root section was determined by electron microprobe (EMPA). The measurements were performed on the right part of the root section separately for dentine and cementum. Using this independent method, average values of $(35.4 \pm 2.1)\%_{m/m}$ and $(34.6 \pm 2.4)\%_{m/m}$ were obtained for Ca in the dentine and cementum, respectively. Utilization of Ca as internal reference element for correction of different ablation rate is possible due to its homogeneous distribution within the entire traced surface with exception of scratches, cracks and root channel. Homogeneous distribution has been discussed and published in our previous paper [30]. In this paper, homogeneity is obvious from EMPA measurement performed on cementum and dentine as well (Fig. 7d). The aforementioned average values corresponding to Ca content in cementum and dentine differ approximately about 2% RSD which is in the extent of calcium content variability in each tooth part (cementum and dentine). Moreover, variability and/or standard deviation of Ca content within the entire sample surface are lower than errors of LA sampling equaled to 7–10% [30]. Using NIST 1486 and calcium as internal reference element, the contents of Zn and Sr in dentine were determined as (190 ± 30) mg kg^{-1} and (381 ± 2) mg kg^{-1}, respectively. The mean value of elemental content was calculated as the median of values obtained with 3700 spots for dentine and 250 values for cementum. LODs estimated using NIST 1486 and spot size analysis were ^{44}Ca 54 mg kg^{-1}, ^{66}Zn 1 mg kg^{-1}, ^{135}Ba 0.3 mg kg^{-1} and ^{86}Sr 0.7 mg kg^{-1}. Limits of detection were calculated as $LOD = 3 \times s_{bkg}/[(I_{isotope} - I_{bkg})/c]$, where s_{bkg} is the standard deviation of the background, $I_{isotope}$ and I_{bkg} are the signal intensities of the measured isotope and background respectively and c is the certified content of element in question.

The overall number of ablated spots was ~8500 due to large sample area (about 2.5 cm × 1.5 cm). The total time per one spot measurement equals to 16 s. Analysis of entire sample should take up approximately 38 h. Fluctuation of the energy and instrumental drift are crucial points of the long-time imaging. For correction of this effect, NIST SRM 1486 was analyzed every 2 h of sample mapping. Signals of isotopes corresponding to elemental content in root section were corrected successively as the bone meal was analyzed. The correction is included into the calculation of elemental content because different parts of sample surface are quantified on temporary response from the bone meal.

Mapping showed elevated zinc content in the cementum, on the outer surface and in association with cracks in the tooth (Fig. 5a and b). These are thought to be artifacts caused by post-mortem changes in the composition of cementum and adherent contamination entering the cracks. The portion of the specimen which was less damaged and better preserved (right side in Fig. 5) showed a decrease in Zn content in four concentric rings corresponding to the visually darker bands laid down in the winter months and higher Zn content in the intervening summer months. These patterns were preserved in Zn/Ca and Sr/Zn ratio maps when the zinc was normalized to the calcium matrix and incorporated strontium (Fig. 5c and d). The areas affected by diagenesis (root channel, cracks) were also clearly visible in these maps and could be easily differentiated from the biogenic patterns that were related to the migratory and dietary changes over the life of this bear. The seasonal banding in the Sr/Zn ratio maps was significantly superior to that in Sr/Ba ratio maps, presumably because barium is more prone to diagenesis which minimizes/maximizes the elemental content inside the dentine [30].

The fluctuation in mentioned ratios reveals the changes in dietary and bear's life territory. Moreover, the content of Zn and Sr in dentine of bear tooth obtained by LA-ICP-MS falls between category of omnivore and carnivore [2]. On basis of this fact we can conclude that bear consumed meat and portion of plants in summer seasons of its life. The same results as were obtained by LA-ICP-MS were acquired by geochemical analysis according to δ^{87}Sr, δ^{13}C and δ^{15}N ratio discussed in sections "Strontium isotopic ratio" and "Carbon and nitrogen isotopic ratio". Quantification

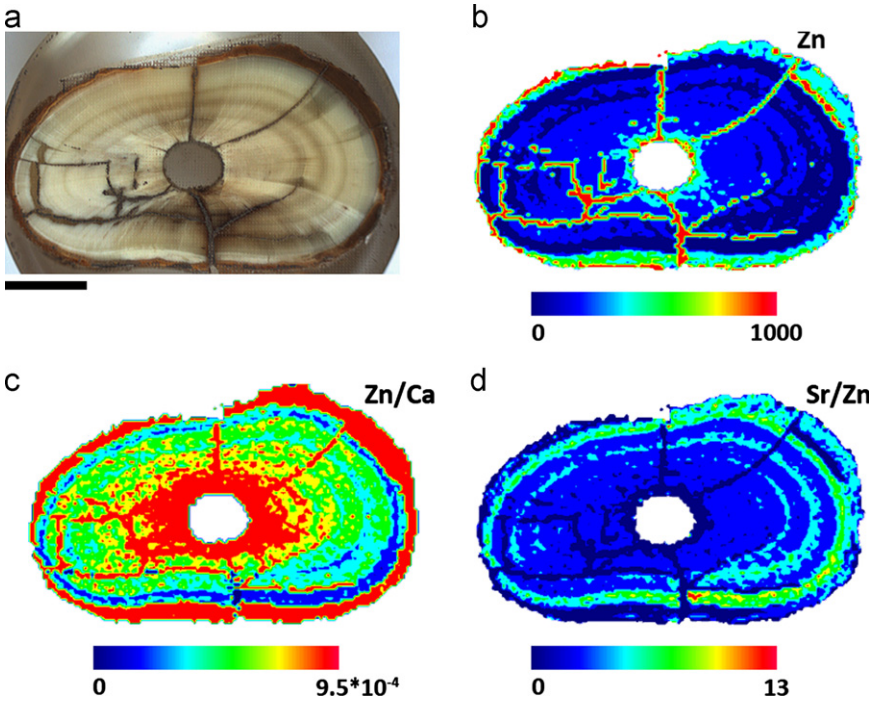

Fig. 5. Ablation pattern is visualized in (a) with a distance of ablation craters of 200 μm and 100 μm in diameter by means of LA-ICP-(Q)MS. Distribution of (b) Zn, (c) Zn/Ca and (d) Sr/Zn across the root section of brown bear's canine tooth is shown. The color scale is in unit of milligram per kilogram (mg kg^{-1}) and the bar has a length of 5 mm.

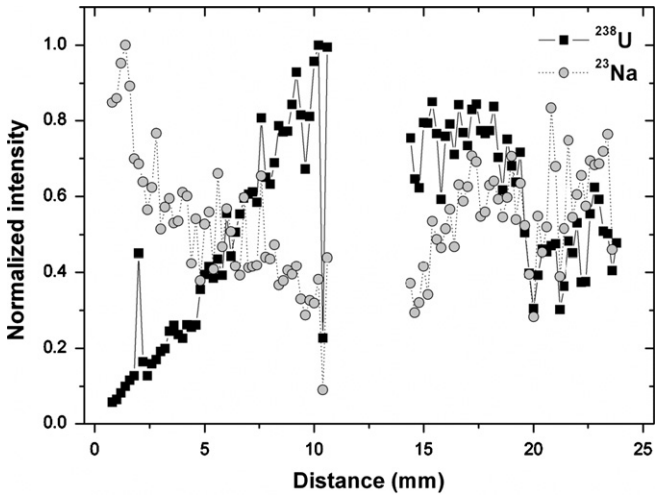

Fig. 6. Distribution of ^{23}Na and ^{238}U along the investigated sample surface obtained by LA-ICP-(Q)MS in hole drilling mode.

Table 2
Content of selected elements in cementum and dentine of canine tooth sample obtained by LA-ICP-(Q)MS.

Element	Content in cementum ($mg\ kg^{-1}$) ± SD	Content in dentine ($mg\ kg^{-1}$) ± SD
Ba	650 ± 70	56 ± 12
Zn	570 ± 200	190 ± 30
Sr	1120 ± 90	381 ± 2

procedure and elemental mapping could together create powerful tools, if diet and migration are investigated for a specific period of the life.

3.5. Diagenesis

The main interpretational problem in the analysis of fossilized archeological samples is identifying artefacts caused by diagenesis. In the case of the bear canine, which is about 28,500 years old, post-mortem changes have clearly occurred, especially where there are cracks and other defects. In Fig. 6, the signal of ^{23}Na isotope, measured in the middle and across the root, is attenuated towards the root channel which indicates leaching during diagenesis. Conversely, the signal of ^{238}U increases as the Na signal decreases indicating possible substitutive events. The mechanism of diagenesis is still not fully understood. However, it is known that the content of elements such as F increases with sample age. Fluorine content in recent teeth is typically in the range of (0.01–0.1)$\%_{m/m}$ [69]. EMP analyses of the bear tooth showed a fluorine content of (0.75 ± 0.15)$\%_{m/m}$ in the dentine and (1.70 ± 0.24)$\%_{m/m}$ in the cementum. Additional evidence for enhanced diagenesis in the cementum is shown in LA-ICP-(Q)MS elemental analyses given in Table 2.

The fluctuations in Mg, Fe, Na and F in the cementum and dentine measured by EMPA are shown in Fig. 7. For orientation, spots "1–5" are located in the cementum with spots 1 and 2 being on the edge of cementum near to the resin and spot 5 being on the cementum dentine interface. A progressive decrease in the fluorine content is visible as one analyses spots closer to the dentine. Spots 6 to 14 are within the dentine and span from close

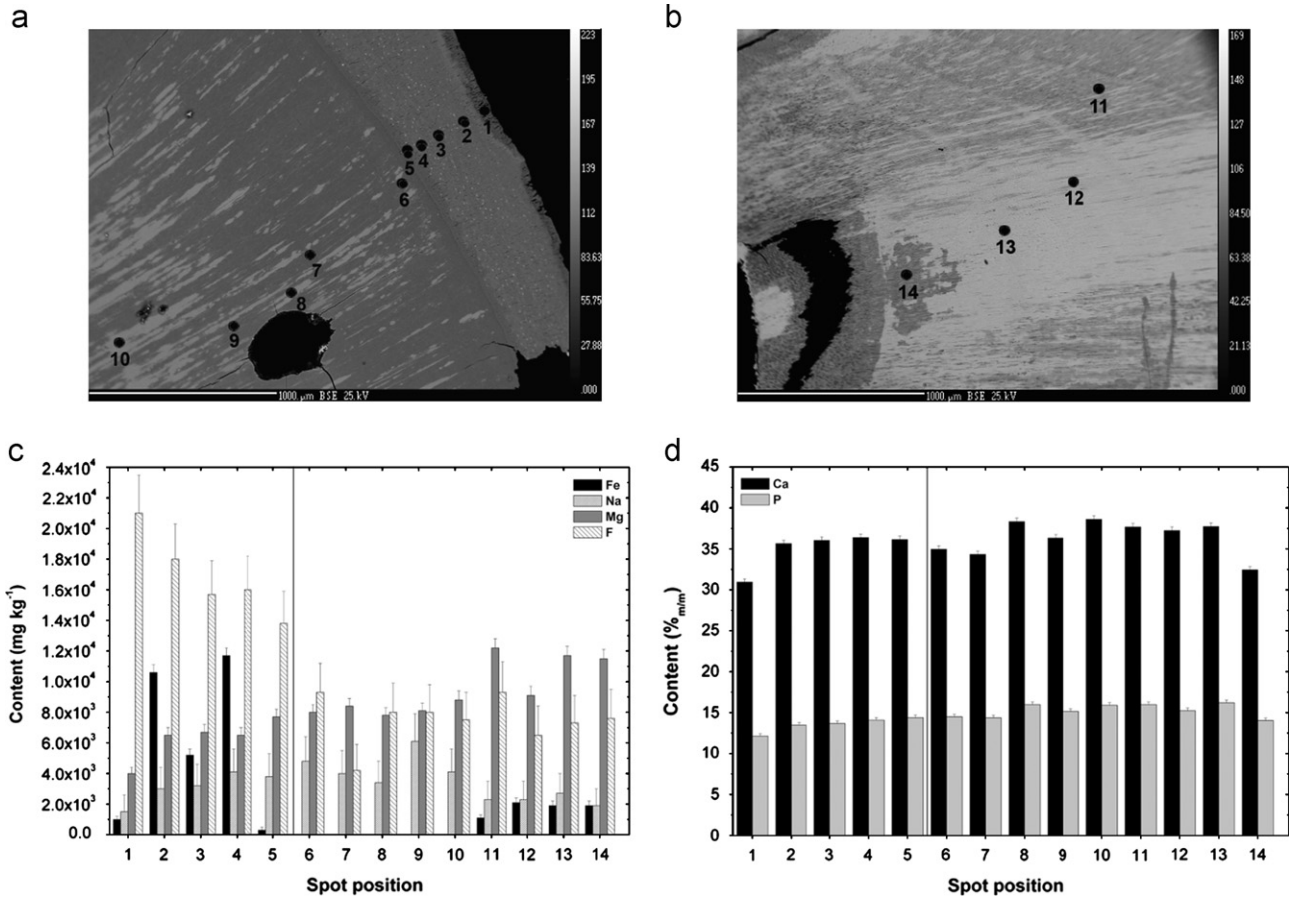

Fig. 7. Photographs: (a) of cementum and dentine and (b) of the dentine near to root channel obtained by BSE. In (a) and (b) spots where levels of elements were measured are shown. Content of (c) Fe, Na, Mg, F and (d) Ca, P obtained by EMPA.

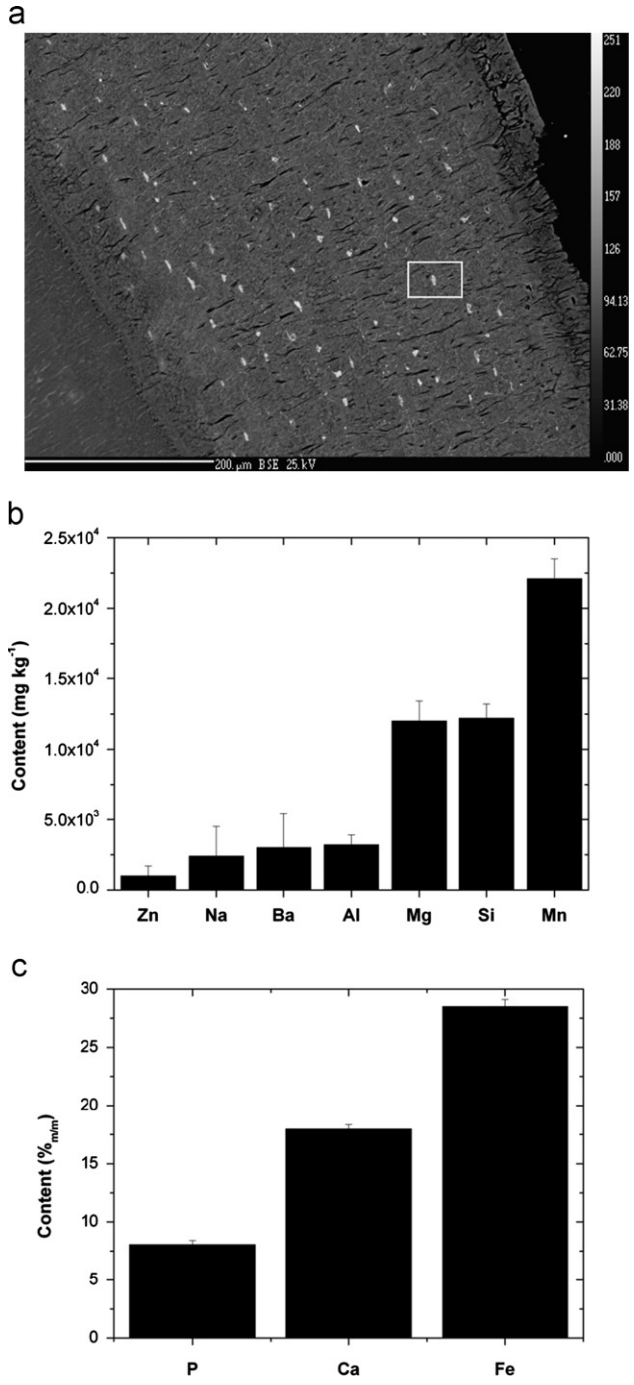

Fig. 8. (a) Detail of cementum obtained by BSE and content of (b) Zn, Na, Ba, Al, Mg, SI, Mn and (c) P, Ca, Fe in small light particles (marked by white rectangle) inside the cementum measured by EMPA.

to the cementum interface to the root channel. Analyses close to the root channel showed reduced sodium and increased Mg and Fe content —possibly due to contamination. Zinc and strontium were below the LOD in the dentine but could be readily detected in the cementum. In contrast, barium was below the LODs in both the cementum and the dentine. The cementum also had discrete particles with a diameter of about 1 μm containing 18.0%$_{m/m}$ Ca, 8.1%$_{m/m}$ P, 28.5%$_{m/m}$ Fe, 2.2%$_{m/m}$ Mn, 1.2%$_{m/m}$ Mg, 0.2%$_{m/m}$ Na and other trace elements indicative of oxides and hydroxides of iron (Fig. 8). Based on LA-ICP-MS and EMP analysis, sample area which is not affected by diagenesis is clearly distinguished and can be used for reconstruction of diet/migration without any chemical intervention enabling reduced post-mortem changes in elemental content.

4. Conclusion

In this work, laser ablation inductively coupled plasma mass spectrometry was used for elemental mapping in a fossil tooth sample having a hydroxyapatite matrix. The same shapes of isotopic intensity and/or ratio were provided using both analyzers. Generally, better precision is achieved by using TOF but precision of Q MS is sufficient for monitoring of elements in skeletal tissue. All the parts of a tooth root can be clearly distinguished together with winter and summer strips inside the dentine. It was observed that migration and diet are better reflected by the Sr/Zn ratio in comparison with Sr/Ba. It is possible to determine the content of elements by using bone meal together with an independent method for the elimination of the different ablation rates of the skeletal remains and the pellet. Quantification procedure and elemental mapping could be efficient for determination of dietary and migration in specific period of the human and animal life. Moreover, diagenesis can be revealed on the basis of the presence of elements that are not normally contained in teeth and bone. With respect to the preliminary study, all results have to be confirmed by geochemical analysis. Finally, verification requires analysis of various types of teeth and bones and an understanding of the mechanisms of diagenesis.

Acknowledgments

The authors acknowledge the AMVIS Agency and Ministry of Education, Youth and Sports of the Czech Republic for support of the Project ME10012 in program KONTAKT, the Czech Science Foundation for Grant 203/09/1394, and the European Regional Development Fund Project "CEITEC" (CZ.1.05/1.1.00/02.0068).

References

[1] L.T. Humphrey, W. Dirks, M.Ch. Dean, T.E. Jeffries, Folia Primatol. 79 (2008) 197–212.
[2] V. Smrčka, Trace Elements in the Bone Tissue, The Karolinum Press, Czech Republic, 2005.
[3] M. Sponheimer, D. de Ruiter, J. Lee-Thorp, A. Späth, J. Hum. Evol. 48 (2005) 147–156.
[4] A. Sillen, J. Hum. Evol. 23 (1992) 495–516.
[5] A. Mays, J. Archaeol. Sci. 30 (2003) 731–741.
[6] H.M. Tvinnereim, R. Eide, T. Riise, Sci. Total. Environ. 255 (2000) 21–27.
[7] J.H. Burton, T.D. Price, J. Archaeol. Sci. 17 (1990) 547–557.
[8] J.H. Burton, T.D. Price, W.D Middleton, J. Archaeol. Sci. 36 (1999) 609–616.
[9] K. Szostek, H. Glab, A. Pudlo, HOMO 60 (2009) 359–372.
[10] R.A. Bentley, J. Archaeol. Method Theory 13 (2006) 135–187.
[11] L.E. Wright, J. Archaeol. Sci. 32 (2005) 555–566.
[12] S.R. Copeland, M. Sponheimer, J.A. Lee-Thorp, P.J. le Roux, D.J. de Ruiter, M.P. Richards, J. Archaeol. Sci. 37 (2010) 1437–1446.
[13] A. Zazzo, M. Balasse, W.P. Patterson, Geochim. Cosmochim. Acta 69 (2005) 3631–3642.
[14] T. Tütken, H. Furrer, T.W. Vennemann, Quat. Int.164–165 (2007) 139–150.
[15] M. Sponheimer, T.F. Robinson, B.L. Roeder, B.H. Passey, L.K. Ayliffe, T.E. Cerling, M.D. Dearing, J.R. Ehleringer, J. Archaeol. Sci. 30 (2003) 1649–1655.
[16] M.P. Richards, S. Mays, B.T. Fuller, Am. J. Phys. Anthropol. 119 (2002) 205–210.
[17] V. Balter, Ch. Lécuyer, Geochim. Cosmochim. Acta 74 (2010) 3449–3458.
[18] T. Tutken, T.W. Vennemann, H.U. Pfretzschner, Palaeogeogr. Palaeoclimatol. Palaeoecol. 266 (2008) 254–268.
[19] A.A.M. Gaschen, M. Doebeli, A. Markwitz, B. Barry, S. Ulrich-Bochsler, U. Kraehenbuehl, J. Archaeol. Sci. 35 (2008) 535–552.
[20] V. Michel, Appl. Geochem. 10 (1995) 146–159.
[21] M.J. Kohn, M.J. Schoeninger, W. Barker, Geochim. Cosmochim. Acta 63 (1999) 2737–2747.
[22] J. Labs-Hochstein, B.J. MacFadden, Geochim. Cosmochim. Acta 70 (2006) 4921–4932.

[23] D. Negrea, C. Ducu, S. Moga, V. Malinovschi, J. Neamtu, C. Ristoscu, I.N. Mihailescu, F. Cornelia, J. Optoelectron. Adv. Mater. 12 (2010) 1194–1199.
[24] E.T. Bergslien, M. Bush, P.J. Bush, Forensic Sci. Int. 175 (2008) 218–226.
[25] T.R. Rautray, S. Das, A.C. Rautray, Nucl. Instrum. Methods B 14 (2010) 2371–2374.
[26] K. Shimada, I. Sato, H. Moriyama, J. Morphol. 211 (1992) 319–329.
[27] A.R. Lodding, P.M. Fischer, H. Odelius, J.G. Noren, L. Sennerby, C.B. Johansson, J.M. Chabala, R. Levisetti, Anal. Chim. Acta 241 (1990) 299–314.
[28] R.J. Speakman, M.D. Glascock, R.H. Tykot, C. Descantes, J.J. Thatcher, C.E. Skinner, K.M. Lienhop, ACS Symp. Ser. 968 (2007) 275–296.
[29] M. Resano, E. Garcia-Ruiz, F. Vanhaecke, Mass Spectrom. Rev. 29 (2010) 55–78.
[30] M. Galiová, J. Kaiser, F.J. Fortes, K. Novotný, R. Malina, L. Prokeš, A. Hrdlička, T. Vaculovič, M. Nývltová Fišáková, J. Svoboda, V. Kanický, J.J Laserna, Appl. Optics 49 (2010) C191–C199.
[31] M. Galiova, J. Kaiser, K. Novotny, J. Novotny, T. Vaculovic, M. Liska, R. Malina, K. Stejskal, V. Adam, R. Kizek, Appl. Phys. A Mater. Sci. Process. 93 (2008) 917–922.
[32] B. Stoll, K.P Jochum, K. Herwig, M. Amini, M. Flanz, B. Kreuzburg, D. Kuzmin, M. Willbold, J. Enzweiler, Geostand. Geoanal. Res. 32 (2008) 5–26.
[33] M.C. Santos, M. Wagner, B. Wu, J. Scheider, J. Oehlmann, S. Cadore, J.S. Becker, Talanta 80 (2009) 428–433.
[34] J. Dobrowolska, M. Dehnhardt, A. Matusch, M. Zoriy, N. Palomero-Gallagher, P. Koscielniak, K. Zilles, J.S. Becker, Talanta 74 (2008) 717–723.
[35] B. Wu, M. Zoriy, Y.X. Chen, J.S. Becker, Talanta 78 (2009) 132–137.
[36] K. Novotny, J. Kaiser, M. Galiova, V. Konecna, J. Novotny, R. Malina, M. Liska, V. Kanicky, V. Otruba, Spectrochim. Acta Part B 63 (2008) 1139–1144.
[37] D.S. Gholap, A. Izmer, B. De Samber, J.T. van Elteren, V.S. Šelih, R. Evens, K. De Schamphelaere, C. Janssen, L. Balcaen, I. Lindemann, L. Vincze, F. Vanhaecke, Anal. Chim. Acta 664 (2010) 19–26.
[38] J. Lear, D.J. Hare, F. Fryer, P.A. Adlard, D.I. Finkelstein, P.A. Doble, Anal. Chem. 84 (2012) 6707–6714.
[39] D.J. Hare, J.K. Lee, A.D. Beavis, A. van Gramberg, J. George, P.A. Adlard, D.I. Finkelstein, P.A. Doble, Anal. Chem. 84 (2012) 3990–3997.
[40] B. Wu, J.S. Becker, Int. J. Mass Spectrom. 323–324 (2012) 34–40.
[41] J.S. Becker, U. Kumtabtim, B. Wu, P. Steinacker, M. Otto, A. Matusch, Metallomics 4 (2012) 284–288.
[42] D. Hare, C. Austin, P. Doble, M. Arora, J. Dent. 39 (2011) 397–403.
[43] M. Arora, D. Hare, C. Austin, D.R. Smith, P. Doble, Sci. Total Environ. 409 (2011) 1315–1319.
[44] C.E. de Barros, L.V.S. Nardi, S.R. Dillenburg, R. Ayup, K. Jarvis, R. Baitelli, J. Coastal Res. 26 (2010) 80–93.
[45] Y.H. Lu, Y. Zhang, Y. Lai, Y.Z. Wang, Acta Petrol Sin. 25 (2009) 2902–2912.
[46] D. Günther, B. Hattendorf, Trends Anal. Chem. 24 (2005) 255–265.
[47] M. Guillong, D. Günther, J. Anal. At. Spectrom. 17 (2002) 831–837.
[48] J. Kosler, M. Wiedenbeck, R. Wirth, J. Hovorka, P. Sylvester, J. Mikova, J. Anal. At. Spectrom.20 (2005) 402–409.
[49] J. Mikova, J. Kosler, H.P. Longerich, M. Wiedenbeck, J.M. Hanchar, J. Anal. At. Spectrom. 24 (2009) 1244–1252.
[50] B.K Kuhn, K. Birbaum, Y. Luo, D. Gunther, J. Anal. At. Spectrom. 25 (2010) 21–27.
[51] J. Koch, D. Gunther, Appl. Spectrosc. 65 (2011) 155A–162A.
[52] N.J.G. Pearce, J.A. Westgate, W.T., Quat. Int. 34–36 (1996) 213–227.
[53] Y.S. Liu, Z.C. Hu, S. Gao, D. Günther, J. Xu, C.G. Gao, H.H. Chen, Chem. Geol. 257 (2008) 34–43.
[54] J.S. Becker, Inorganic Mass Spectrometry: Principles and Applications, John Wiley & Sons, Chichester, 2007.
[55] J. Košler, Proc Geol. Assoc. 118 (2007) 19–24.
[56] D. De Muynck, F. Vanhaecke, Spectrochim. Acta Part B 64 (2009) 408–415.
[57] L.J. Pouchou, F. Pichoir, Microb. Anal. 20 (1985) 104–105.
[58] B. Klíma, Dolní Věstonice II, Université de Liège, Belgique, 1991.
[59] J. Svoboda, Dolní Věstonice II — Western Slope II, Université de Liège, Belgique, 1991.
[60] J.M. McCrea, J. Chem. Phys. 18 (1950) 849–857.
[61] P.M. Richards, J. Montgomery, O. Nehlich, V. Grimes, Antropologie, XLVI (2008) 185–194.
[62] R.M. Nowak, J.L. Paradiso, Walkers Mammals of the World, 4th ed., Johns Hopkins University Press, London, 1983.
[63] J. Clutton-Brock, Mammals, Dorling Kindersley Limited, London, United Kingdom, 2002.
[64] G.V. Hilderbrand, S.D. Farley, C.T. Robbins, T.A. Hanley, K. Titus, C. Servheen, Can. J. Zool. 74 (1996) 2080–2088.
[65] H. Bocherens, M. Fizet, A. Mariotti, Palaeogeogr. Palaeoclimatol. Palaeoecol. 107 (1994) 213–225.
[66] H. Bocherens, Isotopic biogeochemistry and the paleoecology of the mammoth steppe fauna, in: J.W.F. Reumer, J. De Vos, D. Mol (Eds.), Advances in Mammoth research, Proceedings of the Second International Mammoth Conference, Rotterdam, May 16–20 1999, Deinsea 9, 2003 57–76.
[67] 〈http://www.thermofisher.com〉.
[68] M. Hola, J. Kalvoda, O. Babek, R. Brzobohaty, I. Holoubek, V. Kanicky, R. Skoda, Environ. Geol. 58 (2009) 141–151.
[69] Z. Goffer, Archaeological chemistry, Second edition, John Wiley & Sons, New Jersey, 2007.